Synthesis and properties of novel nanocomposites made of single-walled carbon nanotubes and low molecular mass organogels and their thermo-responsive behavior triggered by near IR radiation†

Asish Pal,‡[a] Bhupender S. Chhikara,‡[a] A. Govindaraj,[b] Santanu Bhattacharya*[a] and C. N. R. Rao*[b]

Received 17th December 2007, Accepted 25th March 2008
First published as an Advance Article on the web 11th April 2008
DOI: 10.1039/b719432c

For the preparation of novel organogel–carbon nanotube nanocomposites, pristine single-walled carbon nanotubes (SWNT) were incorporated into physical gels formed by an L-alanine based low molecular mass organogelator (LMOG). The gelation process and the properties of the resulting nanocomposites were found to depend on the kind of SWNTs incorporated in the gels. With pristine SWNTs, only a limited amount could be dispersed in the organogels. Attempted incorporation of higher amounts of pristine SWNTs led to precipitation from the gel. To improve their solubility in the gel matrix, a variety of SWNTs functionalized with different aliphatic and aromatic chains were synthesized. Scanning electron microscope images of the nanocomposites showed that the texture and organization of the gel aggregates were altered upon the incorporation of SWNTs. The microstructures of the nanocomposites were found to depend on the kind of SWNTs used. Incorporation of functionalized SWNTs into the organogels depressed the sol to gel transition temperature, with the *n*-hexadecyl chain functionalized SWNTs being more effective than the *n*-dodecyl chain functionalized counterpart. Rheological investigations of pristine SWNT containing gels indicated that the flow of nanocomposites became resistant to applied stress at a very low wt% of SWNT incorporation. Again more effective control of flow behavior was achieved with functionalized SWNTs possessing longer hydrocarbon chains. This happens presumably *via* effective interdigitation of the pendant chains with the fatty acid amides of L-alanine in the gel assembly. Remarkably, using near IR laser irradiation at 1064 nm for a short duration (1 min) at room temperature, it was possible to selectively induce a gel-to-sol phase transition of the nanocomposites, while prolonged irradiation (30 min) of the organogel under identical conditions did not cause gel melting.

1. Introduction

Since the early nineties, there has been a strong surge in interest in the design of materials of nanometer dimensions because of their numerous interesting properties and applications.[1–3] During this period, different nanomaterials such as zero-dimensional nanoparticles, one-dimensional nanotubes, nanorods, nanowires and two-dimensional nanosheets have been developed due to the various applications envisaged for them. For real life applications, these materials are often mixed with other systems to yield composites that have altered or superior properties compared to the original constituents. Among such materials, carbon nanotubes (CNTs) and carbon nanotube based materials have inspired a number of scientists to look for a range of potential applications.[4–7] Thus, use of CNTs in polymer–carbon nanotube composites has attracted wide attention.[8–10] CNTs with high aspect ratios possess extraordinary mechanical properties (strength and flexibility), as directly measured by transmission electron microscopy, making them ideal for reinforcing fibers in nanocomposites. CNT reinforced composites have been investigated for improving flame-retardant performances, enhanced conductivity,[11] electrostatic charging,[12] optical emitting devices,[13,14] and in lightweight, high strength composites.[15] Very recently, attention has been drawn to the potential utilization of CNTs in biology and medicine. Though living systems are transparent to and are unharmed by near-infrared (NIR) radiation (700–1100 nm), CNTs show NIR laser (1064 nm) driven exothermicity, which renders them useful for cancer therapy,[16,17] gene delivery,[18–21] drug delivery[22–24] and therapeutic applications.[25–27]

Difficulties with molecular level manipulations and the absence of solubility in common solvents impose serious limitations on the use of CNTs. Indeed, as-produced CNTs are insoluble in all organic solvents and aqueous solutions. They can be dispersed in some solvents by prolonged sonication, but precipitation occurs soon after the process is interrupted. On the other hand, it has been demonstrated that CNTs interacts with different classes of compounds.[28–33] Formation of supramolecular complexes allows a means for processing of CNTs toward the fabrication of innovative nanodevices. Among them the polymer–nanotube composites are well studied and known to wrap around the CNTs.

[a]*Department of Organic Chemistry, Indian Institute of Science, Bangalore, 560 012, Karnataka, India. E-mail: sb@orgchem.iisc.ernet.in*
[b]*Chemistry and Physics of Materials Unit, Jawaharlal Nehru Center for Advanced Scientific Research, Jakkur, Bangalore, 560 064, Karnataka, India. E-mail: cnrrao@jncasr.ac.in*

† Electronic supplementary information (ESI) available: Further experimental details and synthesis scheme; IR, TGA and Raman data; FESEM and AFM images; Vis-NIR absorbance spectrum. See DOI: 10.1039/b719432c

‡ These authors contributed equally to this work.

The polymer, especially those with aromatic moieties, interacts with the CNTs since they can impart a π–π stacking with the nanotube walls. A nanotube–PVA [poly(vinylalcohol)] composite can easily be prepared by mixing an aqueous dispersion of nanotubes with an aqueous solution of the polymer and then casting the mixture as a film.[34] Hill *et al.* have solubilized both single-walled carbon nanotubes (SWNTs) and multi-walled carbon nanotubes (MWNTs) by functionalizing with a polystyrene copolymer.[35] Islam *et al.* reported a simple process for solubilization of high weight fraction of SWNTs in water by the non-specific physical adsorption of sodium dodecylbenzene sulfonate.[36] Alternatively, proteins,[37] DNA[38] and such biomolecules are also known to solubilize SWNTs in aqueous solution. Recently, Zheng and co-workers used combinatorial DNA libraries to isolate short DNA oligomers (30–90 bases) that could disperse SWNTs in water.[39] Fukushima *et al.* reported that when SWNTs were mixed with imidazolium ion-based room temperature ionic liquids, the resulting materials transformed into gels.[40,41]

On functionalization with appropriate organic moieties,[42] the solubility of the SWNTs in organic solvents has been shown to improve. Upon oxidation of the side-walls of the CNTs, carboxylic acid groups are introduced. In this process though SWNTs lose some aromaticity the dispersion of the nanotubes becomes slightly easier in polar organic solvents such as methanol.[43,44] It is known that SWNTs functionalized with long lipophilic chains provide relatively stable dispersions in non-polar hydrocarbon type solvents.[45] Though there are a few recent reports of dispersing SWNTs in an oligomeric hydrogel matrix,[46,47] to date, however, nothing is known about incorporation of CNTs into organogels made of low molecular mass organogelators (LMOGs). LMOGs represent an interesting class of soft materials on their own.[48,49] We, therefore, sought to examine whether incorporation of both pristine SWNTs and functionalized SWNTs into LMOGs is feasible and if so what the properties of such resulting nanocomposites would be.

We have previously reported the synthesis and characterization of an efficient gelator (LMOG) based on the fatty acid amide of L-alanine (Chart 1).[50,51] We also showed that the incorporation of gold nanoparticles modulates the properties the gel–Au nanoparticle composites depending on the 'information' inscribed on the nanoparticle surface as capping agent.[52] Herein, we present the results of incorporation of SWNTs, MWNTs and functionalized SWNTs decorated with amides of different chain lengths into the organogel networks, which gives rise to new types of gel–CNT composites. Each composite was characterized by UV-vis and scanning electron microscopy. The thermal stability of the composites was assessed using differential scanning calorimetry. Rheological studies on the composites have provided information about the viscoelastic behavior of the nanocomposites compared to the naked gel. Finally, we have also demonstrated, for the first time, the thermoreversible phase transition properties of such LMOG gel–CNT nanocomposites upon short NIR irradiation.

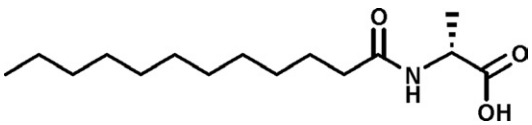

Chart 1 Molecular structure of **1**.

2. Results and discussion

2.1. Functionalized SWNTs (Fn-SWNTs)

The four kinds of functionalized SWNTs (Fn-SWNTs) synthesized differ from each other in their alkyl chain lengths and chain types. The derivatives synthesized are designated as *n*-$C_{16}H_{33}$-SWNT-amide (C_{16}-SWNT), *n*-$C_{12}H_{25}$-SWNT-amide (C_{12}-SWNT), *n*-C_8H_{17}-SWNT-amide (C_8-SWNT) and benzyl-SWNT-amide (Bz-SWNT) having hexadecyl, dodecyl, octyl and benzyl chains respectively. These Fn-SWNTs were characterized by FT-IR, Raman spectroscopy, UV-NIR spectroscopy, thermogravimetric analysis, electron microscopy and atomic force microscopy (ESI†). Raman shifts at 1580 cm^{-1} (D-band) and 150–210 cm^{-1} (radial breathing mode) indicated the presence of the intact carbon nanotube framework (ESI† Fig. S3). Scanning electron microscope images showed the morphology of single-walled carbon nanotubes in all the derivatives and in the acid treated SWNTs (ESI† Fig. S4). This indicated the tubular nature was retained even after functionalization with different amines. The AFM images of the SWNTs showed 600–800 nm long pristine SWNTs (ESI† Fig. S5). Upon oxidation and further functionalization with long chain amines, the nanotubes became shorter (~150 nm) and the aspect ratio became less than that of the pristine SWNTs.

Introduction of alkyl groups on the surface of carbon nanotubes made them more dispersible in organic solvents compared to pristine SWNTs. All the four amide derivatives could be dispersed in chloroform, dichloromethane and toluene. These were, however, less soluble in methanol in which the product precipitated within two minutes. Among the four derivatives, C_{16}-SWNT was more soluble in toluene followed by C_{12}-SWNT and C_8-SWNT. While Bz-SWNT was partially soluble in toluene, it showed a tendency to settle after some time. Thus the solubility of derivatives in toluene followed the order: C_{16}-SWNT >> C_{12}-SWNT > C_8-SWNT >> Bz-SWNT. The UV-vis-NIR spectrum of C_{16}-SWNT was recorded in toluene. The C_{16}-SWNT absorbed in the near IR region (ESI† Fig. S6), a characteristic region for carbon nanotubes. The high absorbance of radiation in the near-IR region by carbon nanotubes is known to originate from electronic transitions between the first or second van Hove singularities of the nanotubes. This indicated the electronic properties were retained even after the functionalization.

2.2. Incorporation of SWNTs in organogel networks

Each of the amide derivatives of SWNTs (0.1 mg) were sonicated in 1 ml of toluene. In another test tube, 10 mg of the gelator was taken in 1 ml of toluene and heated to 50 °C to make it a clear sol. To the sol, varied amounts of the toluene suspension of the SWNTs were added and the mixtures were sonicated for 5 min at 50 °C to ensure complete dispersion of the nanotubes. Upon cooling the mixture to ambient temperature, the gelation process was completed leading to the formation of gel–SWNT composites with different amounts of SWNTs. Different wt% values of pristine SWNTs could also be incorporated in the gel network, but the optimum SWNT concentration was only 0.5 wt%, beyond which the SWNTs tended to precipitate. On the other hand MWNTs were found to be poorly dispersible in the gel network and precipitated after some time. The MWNTs consist

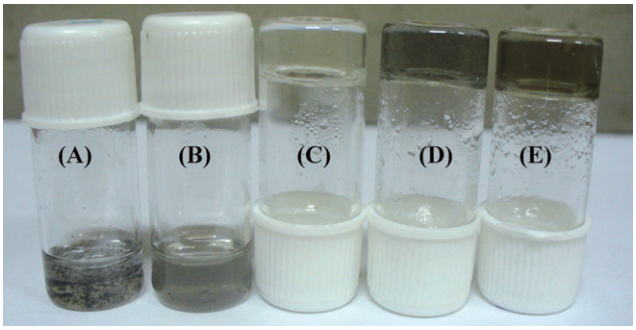

Fig. 1 Photographs showing incorporation of SWNTs in the gel network. (A) Suspension of pristine SWNTs in toluene, (B) C_{16}-SWNTs in toluene, (C) organogel of **1** in toluene, (D) organogel with pristine SWNTs in toluene, (E) organogel with C_{16}-SWNTs in toluene.

of packed concentric nanotubes and have significantly larger diameters than SWNTs. It may be difficult for gelator molecules to efficiently wrap around MWNTs which may explain their poorer dispersibility in the gel than the SWNTs. The Fn-SWNTs having long chain hydrocarbons were found to be much better dispersed in organic solvents. Depending on the relative solubility of the particular Fn-SWNTs in toluene, the dispersion of the nanotubes in the gel network changed. C_{16}-SWNT and C_{12}-SWNT could be loaded as high as 2 wt% and they are stable in the gel network. While C_{16}-SWNT and C_{12}-SWNT having long aliphatic chains could be almost homogeneously dispersed in the gel network (Fig. 1), C_8-SWNT and Bz-SWNT having shorter side-chains produced inhomogeneous gel–SWNT composites.

2.3. UV-NIR spectra of the nanocomposites

When pristine SWNTs were introduced into the gel network the van Hove peak[53,54] could be seen clearly (Fig. 2A). The peaks at 750 and 1000 cm^{-1} were broad in the gel state but more SWNT incorporation resulted in fine structure in the van Hove peaks. Fig. 2B shows visible-NIR spectra of the gel–SWNTs at different temperatures. At 40 °C, *i.e.* above the gel melting temperature, the SWNTs showed the van Hove fine structures but SWNTs impregnated in the gel network showed band broadening.

2.4. Electron microscopy

In order to investigate the microstructures and the morphologies of gel–SWNT composites, SEM analysis was undertaken. SEM images of the gels of toluene showed the existence of three-dimensional fibrillar networks (Fig. 3) but when the pristine SWNTs were incorporated into the gel, the resulting nano-composites showed cluster type morphologies, thus clusters were present in the different domains of the gel network. This indicated that SWNTs did not efficiently disperse in the gel network. With the incorporation of functionalized SWNTs into the organogel network, the fibers coalesced together to form 'collated fibers' of wider diameters and showed densely packed thick networks. The collation of fibers was found to be maximum for C_{16}-SWNT possessing the *n*-hexadecyl chain. The effect became pronounced in the order C_{16}-SWNT >> C_{12}-SWNT > C_8-SWNT. However, the positioning of SWNTs on the gel fibers

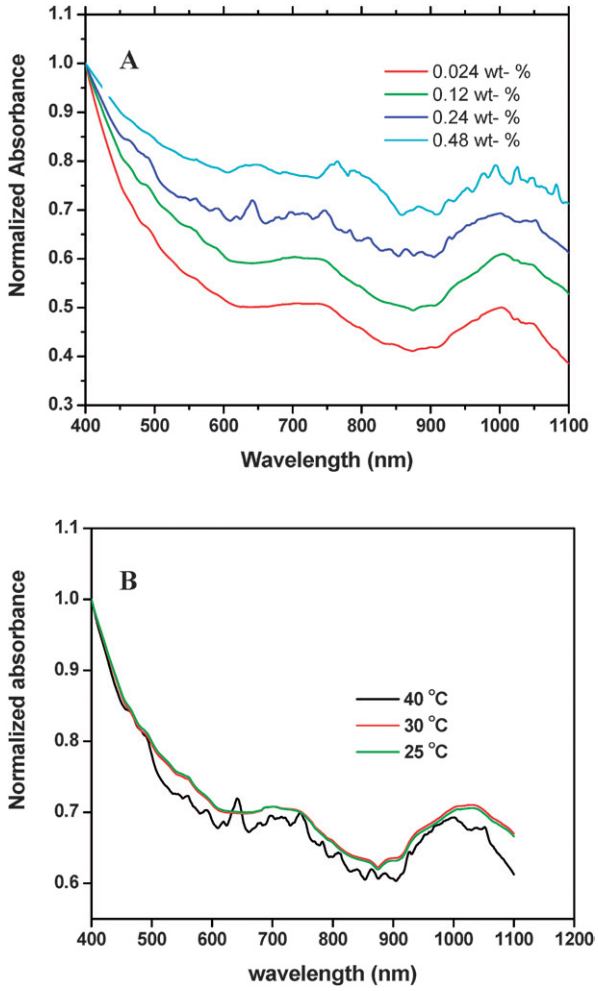

Fig. 2 (A) Visible-NIR spectra of gel–SWNT composites with different wt% of pristine SWNTs at 25 °C. (B) Visible-NIR spectra of the pristine SWNT–gel composite (0.12 wt% pristine SWNTs) at different temperatures. Gel = 10 mg ml^{-1}.

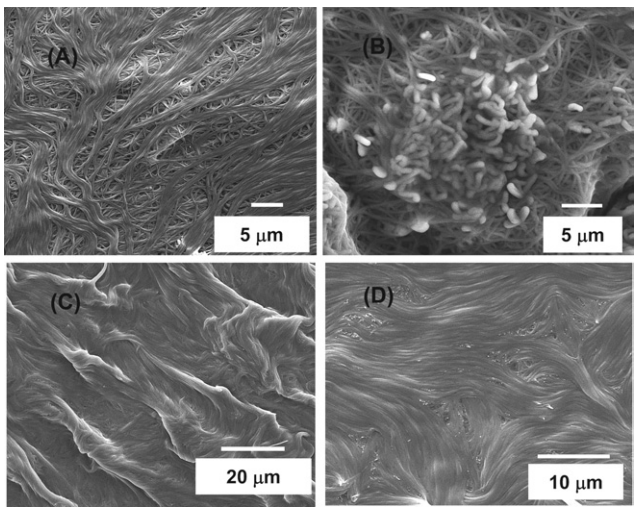

Fig. 3 FESEM images of (A) naked organogel, (B) gel with 0.12 wt% pristine SWNT, (C) gel with 0.12 wt% C_{16}-SWNT, (D) gel with 0.12 wt% C_{12}-SWNT.

could not be ascertained from the SEM images. It is possible that the fibers of the organogel, being of larger dimensions, might wrap the small percentage of individual SWNTs present in the nanocomposites almost completely, the latter being of much smaller dimensions.

2.5. Thermotropic properties of the nanocomposites

To determine the influence of SWNTs on the thermal behavior of the nanocomposites relative to the organogel itself, we first examined the thermal stability of the nanocomposites using differential scanning calorimetry (DSC). However, possibly due to its limited dispersibility and propensity to precipitate during heating and cooling, no significant changes in the thermal properties were observed in the nanocomposites made of pristine SWNTs. In the case of nanocomposites made of Fn-SWNTs the gel formation from the sol showed depression of the gel formation temperatures (T_f) in the DSC cooling scans, although the heating scans did not show any significant changes upon incorporation of Fn-SWNTs. The depression in the gel formation temperature depends on the amount of Fn-SWNT incorporation and the nature of the functional groups on them. Thus, when the same amount (1.98 wt%) of C_{16}-SWNT and C_{12}-SWNT were separately incorporated in the organogel networks of **1**, C_{16}-SWNT with the *n*-$C_{16}H_{33}$ chain caused a greater depression of the sol to gel transition temperature (T_f) (Fig. 4). The organogel alone showed a T_f at 23 °C, while the Fn-SWNT-composite showed a T_f at 18.5 °C. With the comparatively shorter dodecyl chain, the extent of the depression of T_f was found to be less and the composite showed a T_f at 20 °C. C_8-SWNT and Bz-SWNT, due to their lower dispersibility in the organogel phase, separated from the mixture and hence did not produce reproducible results. Also, when the amounts of C_{16}-SWNT and C_{12}-SWNT incorporation were varied we could see changes in the extent of the depression of T_f. With incorporation of more nanotubes in the composites, the T_f for sol to gel transition showed greater depression and this was observed for both C_{12}-SWNTand C_{16}-SWNT (Fig. 5A and B). Increasing depression in the T_f of the nanocomposites indicates more efficient mixing of the SWNTs in the fibrillar networks of the organogel.

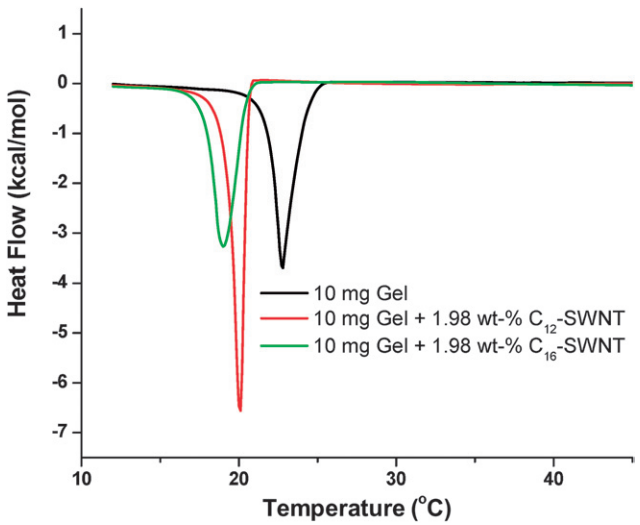

Fig. 4 DSC thermograms (cooling scan) of naked gel, gel with 1.98 wt% C_{16}-SWNT, and gel with 1.98 wt% C_{12}-SWNT.

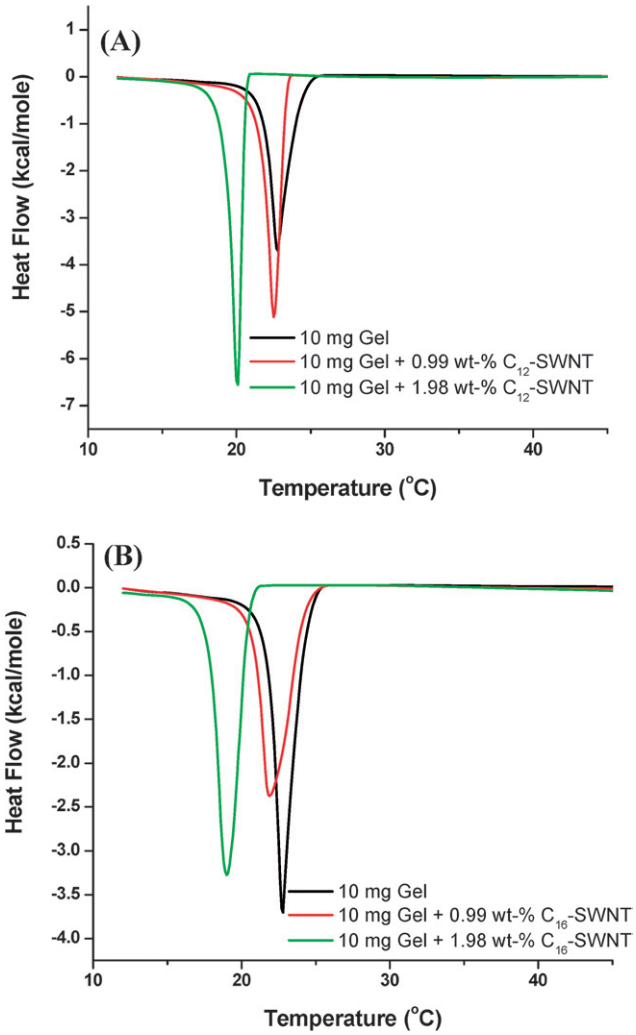

Fig. 5 DSC thermograms (cooling scans) of nanocomposites consisting of (A) C_{12}-SWNT and (B) C_{16}-SWNT at different wt% values in the nanocomposite.

2.6. Rheological studies

We wanted to investigate whether the rheology of the gel was influenced upon incorporation of SWNTs. Rheological studies give an indication about the flow behavior and the rigidity of a gel. In an oscillatory amplitude sweep experiment, (a) G' or the storage modulus represents the ability of the deformed material to restore its original geometry, and (b) G'' or the loss modulus represents the tendency of a material to flow under stress. For viscoelastic materials like gels, G' is an order of magnitude greater than G'', demonstrating the dominant elastic behavior of the system. The yield stress (σ_y) refers to the critical applied stress above which the gel starts to flow. In other words, the property of the gel changes from a dominant elastic-solid like behavior to a dominant viscous-liquid like behavior. Usually this point is determined by measuring the stress value at which G'' becomes larger than G' (in a so-called stress amplitude sweep experiment).

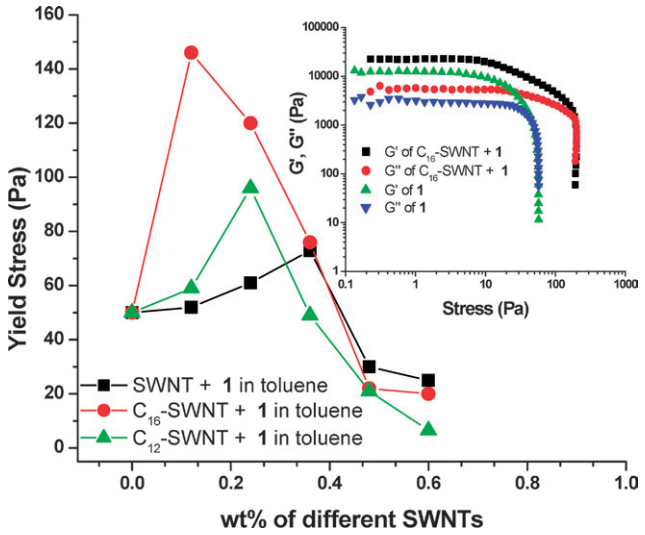

Fig. 6 Plots of yield stress *vs.* wt% of different SWNTs incorporated in the organogels.

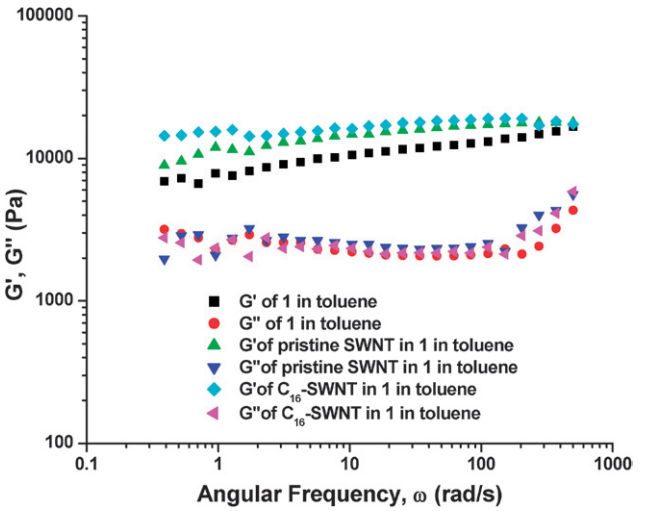

Fig. 7 Typical frequency sweep experiments of the organogels (10 mg ml^{-1}) alone, 0.24 wt% pristine SWNT–gel nanocomposite and 0.24 wt% C_{16}-SWNT–gel nanocomposite.

Each gel has its own particular σ_y according to its strength or rigidity to an oscillating stress.[55–57] Accordingly, the viscoelastic behavior of the 'naked' organogel and the gel–SWNT composites were examined. We observed that the naked gel made in toluene succumbed to the applied stress and began to flow at ~50 Pa (Fig. 6). Incorporation of a small amount of SWNTs (0.2–0.6 wt-%) rendered the gels initially somewhat rigid, but with the incorporation of more SWNTs the yield stress of the composite went down. This suggests that the pristine SWNTs formed nanotube 'clusters' in the gel network which made the organization of the composite micro-heterogeneous rendering its flow easier with the incorporation of higher percentages of pristine SWNTs. In the case of Fn-SWNTs, which are much better solubilized compared to pristine SWNTs in the organogel network, the incorporation of a small amount of Fn-SWNTs (in the range up to 0.24 wt%) in the gel network made the gel more viscoelastic and it started to flow under applied stress at considerably higher than 50 Pa. Hexadecyl functionalized SWNTs made the gel more viscoelastic ($\sigma_y \sim 145$ Pa) than its dodecyl counterpart ($\sigma_y \sim 95$ Pa). So the chain length of the amines attached to the SWNTs becomes crucial in controlling the dispersibility in gel network and hence the viscoelasticity of the gel–SWNT composites. For both C_{16}-SWNTs and C_{12}-SWNTs, with incorporation beyond 0.3 wt%, the yield stresses of the resulting composites became lower. This indicates a less viscoelastic solid-like behavior of the nanocomposites. Thus an optimum loading of Fn-SWNTs in the organogel gives the composite maximum rigidity after which the gel organization gets perturbed and the composite's rigidity starts to decrease.

Gels and gel–SWNT composites were next subjected to frequency sweep measurements under a constant strain of 0.005. It is apparent from Fig. 7 that in the frequency range of 0.1 to 500 rad s^{-1}, both the naked gel and the gel–SWNT composites show elastic storage moduli, G', which are always greater than the associated loss moduli, G''. This type of mechanical behavior is generally a characteristic feature observed in cases of soft viscoelastic solids. The naked gel (10 mg ml^{-1}) shows a frequency dependence of the storage modulus, and at the lower frequency limit it tends to approach towards the crossover of elastic and loss moduli, indicating weak viscoelastic solid-like behavior. Incorporation of SWNTs in both pristine and functionalized form made the composite significantly more viscoelastic solid-like, as both G' and G'' became almost frequency independent over the frequency range 0.1–500 rad s^{-1}. Also, the constant G' value of the gel–C_{16}-SWNT (0.24 wt%) composite was higher than that of the gel–SWNT (0.24 wt%) composite in the above-mentioned frequency range. Here, also the long chain of the C_{16}-SWNTs plays an important role in making the composite more viscoelastic solid-like.

2.7. NIR laser irradiation studies

Recently there have been considerable effort to develop "smart" polymeric and LMOG gels, where environmental stimuli[58–60] such as light or temperature change the physical properties of the gel. Smart gels are important for drug delivery,[61] and have potential therapeutic applications. While UV-vis radiation is harmful for living systems, NIR radiation is transparent and unreactive with biological systems.[26] The SWNTs possess the unique property of laser-driven exothermicity,[39] which can be utilized in developing smart gel–SWNT composites. The toluene gel of **1** and the gel–CNT composites derived from it are shown to be thermoreversible as evident from the differential scanning calorimetry results. The gel–SWNT composites upon NIR laser irradiation exhibited a gel-to-sol transition at 20 °C whereas the control, *i.e.* toluene gel of **1**, did not show any 'melt' at this temperature even after prolonged irradiation at 1064 nm (Fig. 8). The gel–pristine SWNT (0.13 wt%) nanocomposite took ~12 min for the gel-to-sol transition whereas the gel–C_{16}-SWNT (0.13 wt%) composite exhibited a faster gel-to-sol transition (~5 min) upon NIR irradiation. Incorporation of *ca.* 10 times excess of C_{16}-SWNTs (1.35 wt%) in the gel network made the composite more susceptible to NIR irradiation and it exhibited the gel-to-sol transition in ~1 min. In contrast, the naked gels of **1** even after 30 min of continuous laser irradiation did not trigger any gel melting. The nanocomposites after a few minutes of standing

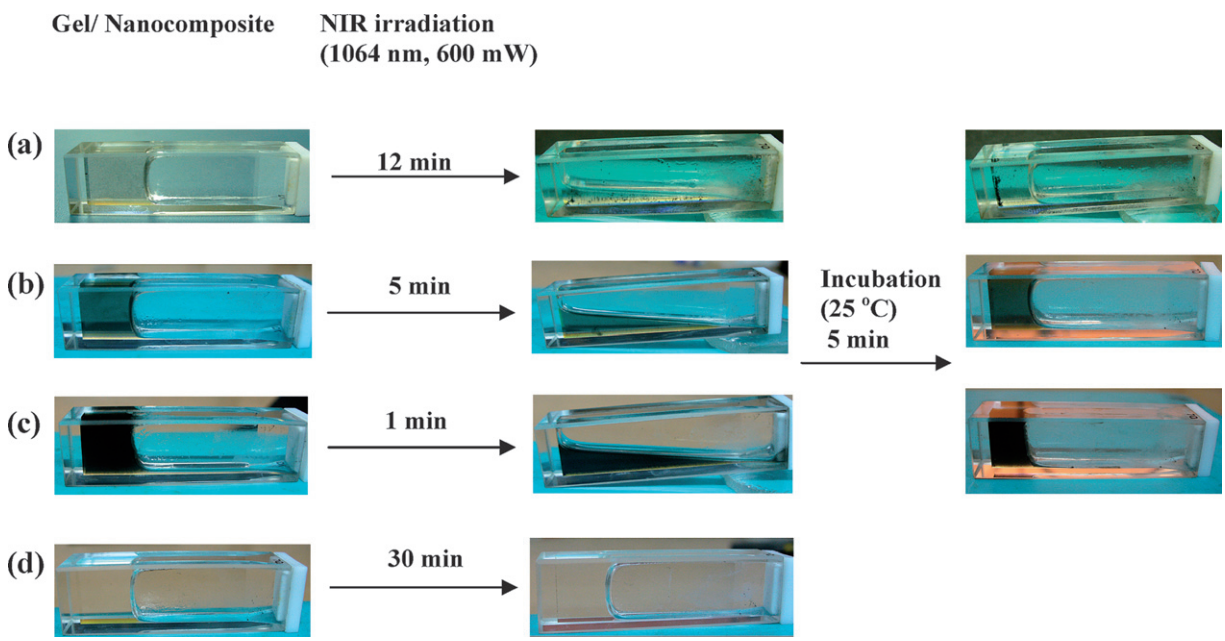

Fig. 8 NIR triggered gel-to-sol phase transitions of SWNT–gel composites at 20 °C: (a) 0.13 wt% pristine SWNT in 15 mg ml^{-1} toluene gel, (b) 0.13 wt% C_{16}-SWNT in 15 mg ml^{-1} toluene gel, (c) 1.315 wt% C_{16}-SWNT in 15 mg ml^{-1} toluene gel, (d) 15 mg ml^{-1} toluene gel.

at room temperature reverted back to the gel state. In the case of gel–pristine SWNT composites, the SWNTs separated partly from the gel network, while the functionalized SWNTs remained homogeneously dispersed in the gel. SWNTs having characteristic van Hove transitions in the NIR region (700–1100 nm) are known to absorb NIR light and become heated due to their high thermal conductivity. The long chain Fn-SWNTs, being almost homogeneously dispersed in the gel network, heated the matrix faster than the pristine SWNTs which are not as well dispersed.

3. Conclusions

We have prepared a new class of nanocomposites based on SWNTs and a LMOG organogel. While the dispersion of pristine carbon nanotubes in the organogel network was possible, increased incorporation led to the precipitation of the former. To improve the loading of CNTs in gels, SWNTs functionalized (Fn-SWNT) with different lengths of hydrocarbon chains were dispersed in the organogel network. Incorporation of enhanced amounts of modified SWNTs altered the thermal and mechanical properties of the gel network significantly. The sol-to-gel phase transition temperature decreased with increasing chain length of the Fn-SWNTs, suggest greater miscibility of such nanotubes in the organogels due to their better ability to induce chain interdigitation. The flow behavior of the nanocomposites was also found to depend on the length of the hydrocarbon chain in the Fn-SWNT. Thus, C_{16}-SWNTs and C_{12}-SWNTs disperse homogeneously in the gel network and the enhanced van der Waals interactions with the long chains of the gel fibers collated the fibrous assemblies of gelator molecules into close-packed aggregates resulting in their greater rigidity as compared to the naked organogel. On NIR laser irradiation, the gel–SWNT composites show a marked gel-to-sol phase transition within a reasonably short time. Thus, we have demonstrated a marked melting transition in the gel–SWNT composites triggered by NIR laser irradiation at ambient temperature, a temperature far below its phase transition temperature. This observation can be exploited to design systems containing SWNTs, which may be potentially useful for triggered materials release or drug delivery.

4. Experimental

4.1. Materials and methods

Single-walled carbon nanotubes (SWNTs) were synthesized by the arc discharge method from graphite and purified by treatment with concentrated HCl acid (to remove iron catalyst) and further hydrogen treatment at 900 °C in a furnace oven as described.[62–64] All other chemicals were obtained from well known suppliers and used as supplied. THF was dried over sodium wire by the usual laboratory methods. Infra-red spectra were recorded on a Perkin Elmer Spectrum BX spectrophotomer. UV-vis-NIR spectra were recorded on a Perkin Elmer Lambda 35 spectrophotometer. For Raman spectra, samples were prepared by depositing a thin film on a glass slide and measured by irradiating with laser light at 632.81 in a Horiba Jobin Yvon instrument. Field emission scanning electron microscopy images were taken with a FEI-Quanta 200 instrument. For atomic force microscopy, SWNT suspensions in toluene were deposited on freshly cleaved graphite sheets and the images were taken in tapping mode using a Dimension 3100 attached with a Nanoscope IV controller. Thermogravimetric analysis was performed on a Mettler Toledo Star System at a heating rate of 5 °C min^{-1}.

4.2. Synthesis

Compound **1**, *N*-lauroyl-L-alanine, was synthesized in high isolated yield and optical purity using a reported procedure.[50,51]

All derivatives of SWNTs were synthesized by adaptation and modification of reported procedures for oxidation of CNTs and amide formation.[65,66] A typical reaction involved introduction of carboxylic acid groups by oxidation of purified SWNTs by refluxing in 3 M nitric acid solution. The acid group was converted into an acid chloride by refluxing in thionyl chloride for 36 h or in oxalyl chloride for 3 h. The excess thionyl chloride or oxalyl chloride was removed under vacuum. Then the coupling of the SWNT carboxylic acid chloride was initiated by addition of the respective alkyl amine in dry THF followed by refluxing over a period of 48 h. The reaction mixture was then filtered through a 0.2 micron teflon membrane and the residue was repeatedly washed with methanol and toluene, ethyl acetate, and petroleum ether to remove any unreacted amines. This afforded a grayish solid product which was characterized by FT-IR, Raman spectroscopy, UV-NIR spectroscopy, thermogravimetric analysis, electron microscopy and atomic force microscopy.

4.3. Gelation

The resistance of the solvent–gelator mixture toward flow under gravity was used as the test of gelation. The gelator (**1**) was heated in a water bath at 50 °C in a test-tube to make the sol containing the toluene solution of functionalized SWNTs form a clear sol. The sol was sonicated for 5 min at 50 °C, and upon cooling under ambient conditions for 30 min formed a gel stable to inversion of the test-tube.

4.4. Differential scanning calorimetry

Organogel and the composite samples in solvents were prepared as mentioned above and their thermotropic behavior was investigated using high sensitivity differential scanning calorimetry using a CSC-4100 model multi-cell Differential Scanning Calorimeter (Calorimetric Sciences Corporation, Utah, USA).

Gels and the gel–SWNT composites were heated to sol and 0.4 ml clear sols were taken into DSC ampoules. The ampoules were cooled, sealed and the gels were allowed to set overnight under ambient conditions. The calorimetric measurements were carried out in the temperature range of 10 °C to 60 °C at a scan rate of 20 °C h^{-1}. At least two to three consecutive heating and cooling scans were performed. Baseline thermograms were obtained using the same amount of solvent in the DSC cells. The thermograms for the gel were obtained by subtracting the respective baseline thermogram from the sample thermogram using 'CpCalc' software provided by the manufacturer.

4.5. Rheological studies

An Anton Paar 100 rheometer using a cone and plate geometry (CP 25-2) was utilized. The gap distance between the cone and the plate was fixed at 0.05 mm. The gel was scooped onto the plate of the rheometer. Stress amplitude sweep experiments were performed at a constant oscillation frequency of 1 Hz for the strain range 0.001 to 100 at 20 °C. Oscillatory frequency sweep experiments were performed in the linear viscoelastic region to ensure that the calculated parameters correspond to an intact network structure. The rheometer has a built-in computer which converts the torque measurements into either G' (the storage modulus) or G'' (the loss modulus) in oscillatory shear experiments.

4.6. NIR laser irradiation

0.4 ml of the organogel and different gel–SWNT samples were taken into a quartz cuvette of path length 1 cm. The samples were irradiated for different lengths of time using a 1064 nm laser (600 mW) in a CW Nd : YAG 1064 nm laser source under ambient conditions.

Acknowledgements

We are grateful to Department of Science & Technology, New Delhi for financial support. B. S. Chhikara thanks DST for a postdoctoral fellowship. We thank Institute Nanoscience Initiative (INI) for SEM. We thank Prof. V. Natarajan and Mr Nandagopal for their help with NIR laser experiment and Prof. A. K. Sood for giving access to the rheology facility in the Physics Department of the Institute.

References

1 M. C. Daniel and D. Astruc, *Chem. Rev.*, 2004, **104**, 293.
2 C. R. Yonzon, E. Jeoung, S. Zou, G. C. Schatz, M. Mrksich and R. P. V. Duyne, *J. Am. Chem. Soc.*, 2004, **126**, 12669.
3 S. Wang, S. Sato and K. Kimura, *Chem. Lett.*, 2003, **32**, 520.
4 S. Iijima and T. Ichihashi, *Nature*, 1991, **363**, 603.
5 W. A. de Heer, A. Chatelain and D. Ugarte, *Science*, 1995, **270**, 1179.
6 A. G. Rinzler, J. H. Hafner, P. Nikolaev, L. Lou, S. G. Kim, D. Tomanek, P. Nordander, D. T. Cobert and R. E. Smalley, *Science*, 1995, **269**, 1550.
7 P. G. Collins, A. Zettl, H. Bando, A. Thess and R. E. Smalley, *Science*, 1997, **278**, 100.
8 H. D. Wagner, O. Lourie, Y. Feldman and R. Tenne, *Appl. Phys. Lett.*, 1998, **72**, 188.
9 R. Dagani, *Chem. Eng. News*, 1999, June, **7**, 25.
10 A. B. Dalton, *J. Phys. Chem. B*, 2000, **104**, 10012.
11 M. J. Biercuk, M. C. Llaguno, M. Radosavljevic, J. K. Hyun and A. T. Johnson, *Appl. Phys. Lett.*, 2002, **80**, 2767.
12 S. A. Carran, P. M. Ajayan, W. J. Blau, D. L. Carroll, J. N. Coleman, A. B. Dalton, A. P. Davey, A. Drury, B. McCarthy, S. Maier and A. Strevens, *Adv. Mater.*, 1998, **10**, 1091.
13 W. A. de Heer, A. Chatelein and D. Ugarte, *Science*, 1995, **270**, 1179.
14 Y. Saito and S. Uemera, *Carbon*, 2000, **38**, 169.
15 D. Qian, E. C. Dickey, R. Andrews and T. Rantell, *Appl. Phys. Lett.*, 2000, **70**, 2868.
16 N. W. S. Kam, M. O'Connell, J. A. Wisdom and H. Dai, *Proc. Natl. Acad. Sci. U. S. A.*, 2005, **102**, 11600.
17 Z. Liu, W. Cai, L. He, N. Nakayama, K. Chen, X. Sun, X. Chen and H. Dai, *Nat. Nanotechnol.*, 2007, **2**, 47.
18 N. W. Kam, Z. Liu and H. Dai, *J. Am. Chem. Soc.*, 2005, **127**, 12492.
19 Z. Zhang, X. Yang and Y. Zhang, *Clin. Cancer Res.*, 2006, **12**, 4933.
20 R. Singh, D. Pantarotto, D. McCarthy, O. Chaloin, J. Hoebeke, C. D. Partidos, J.-P. Briand, M. Prato, A. Bianco and K. Kostarelos, *J. Am. Chem. Soc.*, 2005, **127**, 4388.
21 Z. Zhang, X. Yang, Y. Zhang, B. Zeng, S. Wang, T. Zhu, R. B. Roden, Y. Chen and R. Yang, *Clin. Cancer Res.*, 2006, **12**, 4933.
22 A. Bianco, K. Kostarelos, C. D. Partidos and M. Prato, *Chem. Commun.*, 2005, 571.
23 A. Bianco, K. Kostarelos and M. Prato, *Curr. Opin. Chem. Biol.*, 2005, **9**, 674.
24 M. Prato, K. Kostarelos and A. Bianco, *Acc. Chem. Res.*, 2008, **41**, 60.
25 E. Miyako, H. Nagata, K. Hirano, Y. Makita, K.-i. Nakayama and T. Hirotsu, *Nanotechnology*, 2007, **18**, 475103.
26 M. J. O'Connell, S. M. Bachilo, C. B. Huffman, V. C. Moore, M. S. Strano, E. H. Haroz, K. L. Rialon, P. J. Boul, W. H. Noon and C. Kittrell, *Science*, 2002, **297**, 593.
27 Y. J. Lu, E. Sega, C. P. Leamon and P. S. Low, *Adv. Drug Delivery Rev.*, 2004, **56**, 1161.
28 A. Hirsch, *Angew. Chem., Int. Ed.*, 2002, **41**, 1853.
29 A. Hirsch and O. Vostrowsky, *Top. Curr. Chem.*, 2005, **245**, 193.
30 C. N. R. Rao, B. Satishkumar, A. Govindaraj and M. Nath, *ChemPhysChem*, 2001, **2**, 78.

31 S. Niyogi, M. A. Hamon, H. Hu, B. Zhao, P. Bhowmik, R. Sen, M. E. Itkis and R. C. Haddon, *Acc. Chem. Res.*, 2002, **35**, 1105.
32 G. d. l. Torre, W. Blau and T. Torres, *Nanotechnology*, 2003, **14**, 765.
33 D. Tasis, N. Tagmatarchis, V. Georgakilas and M. Prato, *Chem.–Eur. J.*, 2003, **9**, 4000.
34 M. S. P. Shaffer and A. H. Windle, *Adv. Mater.*, 1999, **11**, 937.
35 D. E. Hill, Y. Lin, A. M. Rao, L. F. Allard and Y. P. Sun, *Macromolecules*, 2002, **35**, 9466.
36 M. F. Islam, E. Rojas, D. M. Bergey, A. T. Johnson and A. G. Yodh, *Nano Lett.*, 2003, **2**, 269.
37 S. S. Karajanagi, H. Yang, P. Asuri, E. Sellitto, J. S. Dordick and R. S. Kane, *Langmuir*, 2006, **22**, 1392.
38 B. Gigliotti, B. Sakizzie, D. S. Bethune, R. M. Shelby and J. N. Cha, *Nano Lett.*, 2006, **6**, 159.
39 M. Zheng, A. Jagota, E. D. Semke, B. A. Diner, R. S. Mclean, S. R. Lustig, R. E. Richardson and N. G. Tassi, *Nat. Mater.*, 2003, **2**, 338.
40 T. Fukushima, A. Kosaka, Y. Ishimura, T. Yamamoto, T. Takigawa, N. Ishii and T. Aida, *Science*, 2003, **300**, 2072.
41 T. Fukushima, K. Asaka, A. Kosakaa and T. Aida, *Angew. Chem., Int. Ed.*, 2005, **44**, 2410.
42 D. Tasis, N. Tagmatarchis, A. Bianco and M. Prato, *Chem. Rev.*, 2006, **106**, 1105.
43 M. A. Hamon, J. Chen, H. Hu, Y. Chen, M. E. Itkis, A. M. Rao, P. C. Eklund and R. C. Haddon, *Adv. Mater.*, 1999, **11**, 834.
44 J. Chen, A. M. Rao, S. Lyuksyutov, M. E. Itkis, M. A. Hamon, H. Hu, R. W. Cohn, P. C. Eklund, D. T. Colbert, R. E. Smalley and R. C. Haddon, *J. Phys. Chem. B*, 2001, **105**, 2525.
45 J. Liu, M. J. Casavant, M. Cox, D. A. Walters, P. J. Boul, W. Lu, A. J. Rimberg, K. A. Smith, D. T. Colbert and R. E. Smalley, *Chem. Phys. Lett.*, 1999, **303**, 125.
46 S. Bhattacharyya, S. Guillot, H. Dabboue, J.-F. Tranchant and J.-P. Salvetat, *Biomacromolecules*, 2008, **9**, 505.
47 M. Yoshida, N. Koumura, Y. Misawa, N. Tamaoki, H. Matsumoto, H. Kawanami, S. Kazaoui and N. Minami, *J. Am. Chem. Soc.*, 2007, **129**, 11039.
48 S. Bhattacharya and S. N. G. Acharya, *Chem. Commun.*, 1996, 2101.
49 S. Bhattacharya and S. N. G. Acharya, *Chem. Mater.*, 1999, **11**, 3121.
50 S. Bhattacharya and Y. K. Ghosh, *Chem. Commun.*, 2001, 185.
51 A. Pal, Y. K. Ghosh and S. Bhattacharya, *Tetrahedron*, 2007, **63**, 7334.
52 S. Bhattacharya, A. Srivastava and A. Pal, *Angew. Chem., Int. Ed.*, 2006, **45**, 2934.
53 I. W. Chiang, B. E. Brinson, A. Y. Huang, P. A. Willis, M. J. Bronikowski, J. L. Margrave, R. E. Smalley and R. H. Hauge, *J. Phys. Chem. B*, 2001, **105**, 8297.
54 N. Nakashima, S. Okuzono, H. Murakami, T. Nakaia and K. Yoshikawa, *Chem. Lett.*, 2003, **32**, 456.
55 O. Bychuk and B. O. Shaughnessy, *Phys. Rev. Lett.*, 1995, **74**, 1795.
56 F. M. Menger and K. L. Caran, *J. Am. Chem. Soc.*, 2000, **122**, 11679.
57 P. Terech, D. Pasquier, V. Bordas and C. Rossat, *Langmuir*, 2000, **16**, 4485.
58 Y. Li and T. Tanaka, *Annu. Rev. Mater. Sci.*, 1992, **22**, 243.
59 Y. Qiu and K. Park, *Adv. Drug Delivery Rev.*, 2001, **53**, 321.
60 C. C. Lin and A. T. Metters, *Adv. Drug Delivery Rev.*, 2006, **58**, 1379.
61 P. K. Vemula, J. Li and G. John, *J. Am. Chem. Soc.*, 2006, **128**, 8932.
62 S. R. C. Vivekchand, A. Govindraj, M. M. Seikh and C. N. R. Rao, *J. Phys. Chem. B*, 2004, **108**, 6935.
63 S. R. C. Vivekchand, R. Jayakanth, A. Govindraj and C. N. R. Rao, *Small*, 2005, **1**, 920.
64 C. N. R. Rao and A. Govindaraj, *Nanotubes and Nanowires*, RSC Publishing, Cambridge, UK, 2005.
65 J. Liu, A. G. Rinzler, H. Dai, J. H. Hafner, R. K. Bradley, P. J. Boul, A. Lu, T. Iverson, K. Shelimov, C. B. Huffman, F. Rodriguez-Macias, Y. S. Shon, T. R. Lee, D. T. Colbert and R. E. Smalley, *Science*, 1998, **280**, 1253.
66 Y. P. Sun, W. Huang, Y. Lin, K. Fu, A. Kitaygorodskiy, L. A. Riddle, Y. J. Yu and D. L. Carroll, *Chem. Mater.*, 2001, **13**, 2864.

